Triel-Bonded Complexes between TrR_3 (Tr = B, Al, Ga; R = H, F, Cl, Br, CH_3) and pyrazine

Mariusz Michalczyk,*[1] Wiktor Zierkiewicz,[1] and Steve Scheiner*[2]

[1] Faculty of Chemistry, Wrocław University of Science and Technology, Wybrzeże Wyspiańskiego 27, 50-370 Wrocław, Poland

[2] Department of Chemistry and Biochemistry, Utah State University Logan, Utah 84322-0300, United States

Abstract

Complexes between TrR_3 (Tr = B, Al, Ga; R = H, F, Cl, Br, CH_3) molecules and pyrazine have been characterized at the MP2 and CCSD(T) levels of theory. The adducts can be grouped according to the type of molecular arrangement. The first situation places the Tr atom in the plane of the pyrazine ring and contains a triel bond to the N lone pair. For the boron complexes the orbital interaction energy is almost equal to the electrostatic component, while the former is only half the latter for Tr= Al and Ga. The two monomers are stacked above one another in the second configuration, which depends to a greater degree upon orbital interaction and dispersion. The former complexes are more strongly bonded than the latter. Interaction energies (E_{int}) for the stronger complexes vary between -50 and -20 kcal/mol for BBr_3 and $Ga(CH_3)_3$ paired respectively with pyrazine. E_{int} is much smaller for the stacked configurations, ranging from -8 for GaF_3 to -1.4 kcal/mol for BF_3. The value of the maximum of the electrostatic potential correlates poorly with E_{int}, attributed in part to monomer distortions upon complexation.

Keywords: π-hole; MP2; MEP; Ab initio calculations; Molecular modeling.

*Correspondence to: mariusz.michalczyk@pwr.edu.pl, steve.scheiner@usu.edu

1. INTRODUCTION

Many chemical and biochemical processes are regulated by a variety of omnipresent noncovalent interactions. A mixture of noncovalent and covalent bonding is responsible for molecular recognition, proton transfer management and the structure and functions of proteins and DNA [1-6]. Among many of the possible noncovalent bonding schemes, triel atoms (B, Al, etc) participate in the interactions of great chemical and biological significance with a variety of Lewis bases [7-10]. A key property of triel species (for example, boron trihalides) is the presence of an unfilled p-orbital on the triel center and the triel ability to be satisfied with only 6 paired electrons [11]. Molecules containing these atoms are thus able to attractively interact with electron-rich moieties by what has come to be called noncovalent triel bonds [12-15].

Another interesting facet of these atoms concerns their electron density distribution when bonded covalently to electron-withdrawing substituents. A region of electron density depletion, labelled a"π-hole", is located perpendicular to the molecular plane of trivalent triel compounds TrR_3 [16-19]. The features of these π-holes are affected primarily by the size and polarizability of the triel atom and the electron-withdrawing abilities of its R substituents [20-22]. In fact, many of the principles governing these π-holes mimic those earlier determined for their σ-hole counterparts [23-26]. In either case, the intensities of these holes are commonly assessed by analysis of the molecular electrostatic potential (MEP) [23-25]. Both π and σ holes are considered to be principle factors in the origin, nature and properties (e.g., directionality in π-hole complexes [27]) of a large number of noncovalent interactions, including halogen, chalcogen, pnicogen, tetrel and even aerogen bonds [28-33].

The triel bond has been the subject of numerous quantum chemical and experimental studies [12,13,34-48] in recent years. Most of this work agrees that these bonds can be quite strong, bordering on covalency. There is an exceptionally high degree of charge transfer from one molecule to its partner, and the electron densities at the bond critical points (BCPs) are quite large. Grabowski found, for example, that the triel-nitrogen bond strength reaches more than 23.9 kcal/mol, leading to the characterization that "the triel center may be considered as the tetravalent one where the octet rule is obeyed" [12]. Monosubstituted BH_2X (X=F, Cl, Br, I) molecules contain both π- and σ-hole regions [39] and can consequently form stable homodimers. Other work has demonstrated that Si-H···B interactions can stabilize silicon-boron complexes [49-51]. There are also examples of charged-assisted triel bonding interactions in the

context of solid state chemistry [37]. In common with other sorts of noncovalent bonds, triel bonds can be strengthened via cooperative effects from other interactions such as halogen or pnicogen bonds [52,53], manifested in part by contraction of triel bond distances upon trimerization. Other calculations of BX_3 (X=F, Cl, Br) complexes with CH_3CN or HCN exhibited two different geometries, with distinct interaction energies and B···N distances [54-56]. In an interesting potential future application, boron-amine dimers represent one of the first stages of molecular hydrogen release and therefore are a target in the development of new hydrogen storage materials [57,58].

There are a number of outstanding questions that bear detailed scrutiny. In a general sense, are there fundamental distinctions between the triel bond, with its electron deficient triel atom, and other related noncovalent bonds such as H-bonds, or halogen and tetrel bonds? One might expect certain differences as the latter typically involve σ-holes while the triel atom is characterized by a π-hole. How does the strength and other properties of the triel bond vary as one scans down the triel column of the periodic table; is there a regular pattern? It is also important to determine the effects of different substituents on the triel atom, and to examine whether these effects are sensitive to the nature of the central atom. Can one predict substituent effects solely on the basis of electron-withdrawing potency? Some of the most common substituents are halogen atoms which are themselves capable of engaging in noncovalent bonds with an approaching nucleophile. How do these halogen bonds compare in strength with the triel bonds to the same nucleophile? Since the triel atoms are electron deficient, with only three substituents, can they engage in a fourth covalent bond with a sufficiently strong nucleophile, and how might such bonds be predicted in advance? Given the fact that the most positive region of the electrostatic potential is a π-hole, lying directly above the molecular plane, would a nucleophile containing an extended π-system prefer to stack above the triel molecule, i.e. in a parallel arrangement? Another issue has to do with the deformation of the Lewis acid caused by complexation with the base - how might such distortion affect the strength and nature of the binding? It is the goal of the present study to provide answers to these questions, and act as a guide in our conceptualization of triel bonding.

2. SYSTEMS AND METHODS

The three triel atoms Tr=B, Al, and Ga were considered in this study. The three H atoms in their trivalent planar TrH_3 molecules were replaced systematically by substituents R of varying electron-withdrawing capability F, Cl, Br, and Me. Pyrazine was taken as the common Lewis base for a number of reasons. In the first place, in addition to its biological significance [59] it contains a N atom with a single clearly defined lone pair. Its aromatic ring offers the option for it to stack directly above the TrR_3 molecule, which permits comparison with the classic triel bond to the N lone pair. For each combination of a Lewis acid TrR_3 with pyrazine, the entire potential energy surface was searched for all minima, including not only those indicated above, but any others that might be present.

The geometries of the heterodimers and their constituent monomers were fully optimized at the MP2 level of theory in conjunction with the aug-cc-pVDZ basis set [60,61]. Optimized structures were verified as true minima by the absence of any imaginary frequencies. Molecular electrostatic potentials (MEPs) were calculated and extrema on the 0.001 au electron density isosurface were determined at the MP2/aug-cc-pVDZ level using the WFA-SAS program [62]. Interaction energies (E_{int}) of complexes were obtained at both the MP2 and CCSD(T) [63] levels, both with aug-cc-pVDZ, to probe the reliability of the former. The basis set superposition error (BSSE) was corrected by the counterpoise (CP) procedure [64]. The Natural Bond Orbitals (NBO) technique implemented in the 5.0 version of the GenNBO software was used to study the interorbital interactions and charge transfer [65]. NBO were performed at the BLYP-D3(BJ)/def2TZVPP level [66] of theory. AIM analysis [67] elucidated the positions of bond paths and their corresponding bond critical points (BCPs). This view was further elaborated via the NCI (noncovalent index) procedure using MultiWFN and the VMD suite of programs [72-74]. The interaction energies were dissected into their components via Morokuma-Ziegler EDA (Energy Decomposition Analysis) methodology at the BLYP-D3/ZORA/TZ2P level [68-71] using ADF [68-70] package. All remaining computations which did not require external software were carried out with the Gaussian09 [75].

3. RESULTS

3.1. Structures and electrostatic potentials of isolated monomers

The molecular electrostatic potential maps of isolated AlR_3 molecules, representative of all TrR_3, are presented in Fig. 1 where red coloured regions represent positive potential, and negative regions are shown in blue. There is a red π-hole located above (and below) each Al atom, with negative regions on the periphery of the molecule. The red region is a bit larger for the AlH_3 and AlF_3 molecules. When F=Cl or Br the π-holes are smaller but σ-holes, albeit weak ones, appear on the extensions of the Al-R bonds. In the case of $Al(CH_3)_3$, the positive regions are associated with the methyl groups, most notably their H atoms.

[Insert Fig. 1 here]

These various positive holes can be quantified via elucidating the maxima of the MEP on an isodensity surface, in this case with ρ=0.001 au. These quantities are reported as $V_{s,max}$ for all three Tr atoms in the upper half of Table 1 and are consistent with the patterns in Fig. 1. Replacement of H by the strongly electron-withdrawing F increases $V_{s,max}$ whereas it is diminished for the electron-releasing methyl group. Br also reduces this quantity, although not by as much as methyl. The effects of chlorosubstitution are mixed, depending upon the identity of the triel atom. While enlargement of Tr from B to Al enhances the π-hole as might be anticipated [76,77], further enlargement to Ga acts in the opposite manner, reducing $V_{s,max}$. This trend may be associated with the atom electronegativity which is greater for Ga (1.81) as compared to Al (1.61). The greater importance of electronegativity vs atom size is consistent with an earlier study of tetrel bonds [78]. These various patterns combine to yield the most intense π-hole for AlF_3, and the weakest for $B(CH_3)_3$. Note parenthetically, that there is a large gap between R=F and any other substituent.

For those molecules that contain a secondary maximum, i.e. σ-holes for R=Cl, Br, or CH_3, these quantities are displayed in parentheses in Table 1. Note that these holes are very much less intense than the π-holes. The largest of these σ $V_{s,max}$ occurs in BBr_3, but this value of 14.3 kcal/mol is still much smaller than the π-hole over the B, despite the weakness of the latter relative to the π-holes of any of these molecules in Table 1. The MEP of the electron donor molecule pyrazine is also illustrated in Fig. 1. As reported earlier [79] its minimum occurs in the

lone pair region of each N atoms, with a value of -29.6 kcal/mol. Note that it does not contain a minimum directly above the aromatic plane.

[Insert Table 1 here]

3.2. Tr··N Triel Bonds to N lone pair

3.2.1 Geometries and interaction energies

When matching the most positive region of each TrR_3 with the most negative of pyrazine, one would expect the strongest interactions ought to arise for geometries of the type illustrated in Fig. 2 for TrH_3 and $TrMe_3$, where the Tr atom directly approaches the N lone pair, i.e. the Tr atom lies in the pyrazine plane. (Geometries of the remaining complexes of this type are illustrated in Fig. S1.) Selected intermolecular geometric parameters are collected in Table 2, along with the most important energetic quantities.

[Insert Fig. 2 here]

[Insert Table 2 here]

For each of these complexes, the R(Tr··N) distance is much shorter than the sum of the van der Waals radii (3.47, 3.39, and 3.42 Å, for B···N, Al···N and Ga···N respectively), one indication of an attractive interaction. While the Tr··N distances for Al and Ga are all longer than 2.0 Å, with R slightly longer for Ga than for Al, the corresponding distances are much shorter for B, less than 1.7 Å. With respect to substituents, for Tr = Al and Ga, the distances are consistent with the idea of shorter distances for more electron-withdrawing substituents: R= F < Cl < Br < H < Me,. This pattern is different for Tr=B, nearly the reverse in that R=Br has the shortest contact, with R increasing for H, Cl, F, and Me in that order. As may be noted from the final column of Table 2, the Tr atom lies within just a few degrees of the projected direction of the N lone pair, consistent with the position of the minimum in the MEP of pyrazine.

The magnitude of the interaction energies of the complexes varies from a minimum of 20 kcal/mol up to a maximum of 50 kcal/mol. In keeping with the dependence of R(Tr··N) upon substituent, methyl groups yield the weakest interactions followed by H, Br, Cl and F in that order. But this pattern holds only for Al and Ga. For Tr=B, the strongest interaction arises with

BBr_3, followed by R= Cl > F > H > Me. Adducts with Tr=Al are more strongly bound than their Ga counterparts, consistent with the more intense π-holes for the former. But B again presents an exception. Despite its relatively weak π-holes, BR_3 consistently engages in the most strongly bound heterodimers.

The third column of Table 2 offers verification of the reliability of the MP2 means of incorporating electron correlation. The interaction energies computed at the higher CCSD(T) level are slightly smaller than those calculated at the MP2 level. This trend is amplified a bit with the halogenated molecules, but still remains at about 10% or less.

Also included in Table 2 are the deformation energies, E_{def}, defined as the energy required to distort each TrR_3 Lewis acid from its optimized structure to that which it adopts within the context of the dimer with pyrazine. These deformations include not only changes of the r(Tr-R) bond length, but also a pyramidalization of the molecule from its normally planar geometry. Consistent with both their stronger interaction energies, and shorter R(Tr··N) distances, the boron complexes exhibit the greatest deformation energies, between 13 and 26 kcal/mol. In fact, there is a clear correlation between the magnitude of this deformation energy and the interaction energy itself, both obeying similar patterns.

When proper account is taken of this deformation energy, one arrives at ΔE for the association reaction, which takes one from the fully optimized monomers to the complex. These quantities are reported in the fifth column of Table 2 and are of course all less negative than E_{int}. Note, however, that ΔE displays certain different trends than does the pure interaction energy between pre-deformed subunits. Most notably, the full ΔE is not necessarily uniformly larger for B than for Al and Ga. Indeed, with the single exception of BH_3, the other BR_3 systems have a less negative ΔE than do their AlR_3 and GaR_3 analogues.

Earlier work [78,80] has demonstrated that geometrical distortions of the sort undergone by the TrR_3 molecules may perturb the MEP, and alter the intensity of the σ or π-hole, and thereby modify the electrostatic portion of the interaction. This effect was examined here by comparing the values of $V_{s,max}$ in the undistorted Lewis acids in Table 1 with the same quantity calculated after the monomer has undergone the deformation required in the optimized dimer. These latter maxima are shown in the lower half of Table 1 and document that, like some of the systems studied earlier, the rearrangement of the Lewis acid caused by complexation with pyrazine intensifies the π-hole maximum substantially. This magnification ranges from a factor of 1.2 all

the way up to 2.4. As the final point, it might be noted that there are issues of inconsistency between $V_{s,max}$ and E_{int} here, not unlike a number of other works in the literature [78, 80-83].

3.2.2 Sources of Binding

As a first step in determining the most important factors in the triel bonding, the total interaction energy was decomposed into its constituent elements via the EDA scheme. The results of this decomposition are explored in Table 3.

[Insert Table 3 here]

As a preliminary point, despite a difference in formulation, the DFT-EDA interaction energies obey the same trends as those calculated at supermolecular MP2 and CCSD(T) levels. The data immediately provide a clear distinction. In the case of the B-containing systems, orbital interactions make an approximately equal contribution as does E_{elec}. But the latter Coulombic forces are considerably larger than E_{oi} for both Al and Ga systems. (Dispersion provides only a small increment in either case.) These patterns can be easily visualized via the pie charts of Fig. S2. The closer contact between the pair of monomers for BR_3 leads to much greater Pauli repulsive forces as compared to Al and Ga.

One can further dissect the nature of the orbital interactions via an NBO analysis. There is first of all the total charge being transferred from the pyrazine base to the Lewis acid, which is defined as CT in Table 4.

[Insert Table 4 here]

More refinement arises by examining transfers between individual orbitals. The N lone pair is the primary source of this transfer. Some of its density is transferred to the σ* antibonding orbitals of the three Tr-R bonds. But a much larger amount moves into the vacant p-orbital of the Tr atom, defined as LP*(Tr) by NBO. The orbitals involved, and their interactions, can be seen explicitly in Fig. S3. The energetic consequences of each such transfer are measured by a perturbative E(2), listed in Table 4. Consistent with the energy partitioning, the NBO results confirm a much higher degree of charge transfer for Tr=B, as compared to Al and Ga. The bulk of this charge is transferred into the vacant p-orbital of the Tr atom. The correlation between

these measures of charge transfer and interaction energy are fairly strong but not perfect, unsurprising in view of the fact that E_{oi} makes up less than half of the total.

When seen in tandem, these results lead to the following conclusion: Within these triel-bonded complexes there are two mechanisms of complexation. The boron complexes rely to a high degree on orbital interactions, roughly equal to the electrostatic term, and involves a good deal of deformation of the Lewis acid geometry. The Al and Ga complexes are more typical of π/σ- hole interactions, which depend in large part on electrostatic forces, with more modest monomer deformation. Therefore, the MEP analyses are in good agreement with E_{int} within these groups of complexes: The Al dimers are more stable than their Ga counterparts, and the substituent order is similar to that obtained by MEP analysis.

Another window into the underlying sources of the bonding derives from AIM treatment of the topology of the total electron density. The molecular diagrams associated with this analysis of the representative Al dimers are depicted in Fig. 3 where small green spheres indicate the location of each bond critical point.

[Insert Fig. 3 here]

The AIM descriptors (electron density, Laplacian of the electron density and total electron energy) of these critical points are gathered in Table 5. It may be noted first from Fig. 3 that several of the dimers, e.g. $AlCl_3$ and $Al(CH_3)_3$, show bonds in addition to the Al··N bond path. However, the data in Table 5 indicates these secondary bonds are considerably weaker. For example, $\nabla^2\rho$ for the two Cl··H bonds in $AlCl_3$···pyrazine amount to only some 10% of the same quantity for the triel bond. One can conclude therefore that the energetics of these complexes are derived almost exclusively from triel bonding.

[Insert Table 5 here]

The AIM data in Table 5 agree with the prior analytics that the B··N bonds are quite a bit stronger than their Al··N and Ga··N sisters. The negative values of H are commonly ascribed to bonds that have at least partial covalent character [84,85], in line with the energetic strength of these bonds. ρ and $\nabla^2\rho$, like H, offer further commonality with the energetics. For instance, ρ_{BCP}

lies in the range of 0.090-0.119 au in BR_3 complexes, while the same parameter is only 0.039 - 0.051 au for AlR_3. The comparison is similar for $\nabla^2\rho$: 0.352-0.613 au for the former and 0.252-0.335 au for the latter. However, the trends are less clear in the comparison between Al and Ga. The stronger bonds of the former are only partially confirmed by $\nabla^2\rho$, while ρ obeys an opposite trend. It might also be noted that the values of H are positive for the Al··N bonds, but negative for their Ga counterparts, which night suggest more covalent character for the Ga bonds. These anomalous patterns raise doubts concerning the ability of the AIM analysis of the wave function to accurately reflect energetics.

3.3 Stacked complexes

3.3.1 Geometries and interaction energies

The strongly negative region of the MEP in the position of the pyrazine N lone pair extends above and below the molecular plane so the positive potential around the triel atom can be attracted to this area as well. This attraction leads to the stacked dimers illustrated in Fig. 4 which are much less strongly bound than the triel-bonded complexes involving the N lone pair (complexes for the TrX_3 heterodimers are displayed in Fig. S4). As displayed in Table 6, the binding energies of these stacked structures are reduced when compared to the lone pair geometries by a factor that varies between 5 and 33.

[Insert Fig. 4 here]

[Insert Table 6 here]

In part due to the weaker nature of the bonding, and the more distant contacts, the deformation energies are much smaller in the stacked structures, no more than about 2 kcal/mol. Consequently, the binding energies ΔE are fairly similar to the interaction energies. It is interesting to note a tight correlation between the deformation energy and interaction energy; the correlation coefficient between these two quantities is 0.93.

Unlike the lone pair dimers discussed earlier, the BR_3 molecules engage in weaker stacking interactions than do their Al and Ga counterparts. For the latter two triel atoms, one sees a binding pattern related to R as F > Cl > Br > Me > H. However, this pattern is completely different for B where it is F that forms the weakest dimer and Me the strongest. In keeping with

their weaker character, the R(Tr··N) distances are quite a bit longer as well. This elongation relative to the planar structures varies from 0.5 Å to as much as 1.5 Å.

A closer examination of the geometries of these complexes places the Tr atom more nearly above a pair of C atoms, rather than directly above N where the MEP might direct the nucleophile. In the case of BH_3··pyrazine for example, the B atom is situated nearly equidistant at 2.68 Å from the two C atoms indicated in Fig. 4, much closer than its 3.25 Å distance from either N atom. As another measure of the structure of each stacked complex, the last column in Table 6 reports the distance between the Tr atom and the midpoint of the relevant C-C bond. These latter distances are clearly shorter than the R(Tr··N) distances, emphasizing the displacement of the triel atom from the negative potential above the N atoms. There are certain patterns that the lone pair and stacked complexes share. For both Tr= Al and Ga, the intermolecular distances vary in the order R=F < Cl < Br < H < Me. On the other hand, while these distances are shorter for Al than for Ga for the lone pair dimers, this order is reversed for R(Tr···C-C) of the stacked geometries.

3.3.2 Analysis

Energy decomposition of the stacked dimers presented in Table S1 shows some important differences with the lone pair structures. Most obvious is the much stronger dispersion component, making up more than 50% of the total attractive force in some cases. In most of the stacked dimers, the orbital interaction plays the major role, with electrostatics roughly comparable to dispersion. Taking the BH_3···pyrazine complex as an interesting example, the orbital interaction contributes 47% of the total attractive force. Surprisingly, when the H atoms are replaced by F, Cl, Br or Me the orbital interaction contribution plunges (from 47 to 18-25 %) and dispersion doubles (from 26 to 56 %).

Rather than the pyrazine N lone pair acting as the primary source of electron transfer, this role is played in the stacked structures by one of the π(C-C) bonding orbitals. The perturbation energy associated with this transfer into the Tr p-orbital (LP* in NBO parlance) is reported in Table S2 where it is immediately obvious that it is far smaller than the corresponding quantities for the lone pair structures in Table 4. Taking the Al series as an example, E(2) for the stacked dimers are in the 3 - 41 kcal/mol range, while the values for the lone pair structures vary between 62 and 100 kcal/mol. This difference is even more stark for Tr=B. Moreover, these is no real correlation between E(2) and the binding energies.

The AIM diagrams of the stacked dimers are a bit more complex than those of the more strongly bound lone pair structures. Some sample diagrams are displayed in Fig. 5 for the Al family.

[Insert Fig. 5 here]

All of them, with the exception of R=Me, contain a bond path that connects Al to one of the pyrazine C atoms, suggesting a Al··C interaction (triel bond). ~~One of the Cl atoms of $AlCl_3$ is connected to another pyridine C atom, in what might loosely be described as a C··Cl tetrel bond.~~ $AlBr_3$ is similar except that the path leads to a C-C bisector, rather than to a single C atom. The AlMe3 diagram is more complex, replacing the Al··C path with a number of others, including C··C and H··C. It is only in the cases of the unsubstituted BH_3 and GaH_3 that bond paths lead from Tr to the center of a pyrazine C-C bond.

The complexity of the AIM diagrams and the numerous specific bond paths are plain in Table S3 which contains numerical values for all of the stacked dimers. These quantities are all quite small, consistent with their weaker nature. In terms of triel bonds, the majority of relevant bond paths connect Tr with a single C atom of pyrazine. Specific connection with a C-C bond was observed only for BH_3 and GaH_3.

As a valuable supplement to the AIM procedure, the noncovalent interaction (NCI) scheme introduced by Yang *et* al. [86-89] has found use in the examination of specific regions of the intermolecular region. NCI is based on the relationship between electron density (ρ) and the reduced density gradient (RDG) generated from the density and its first derivatives [86-89]. The value of ρ determines the strength of interaction. The sign of λ_2 (the second eigenvalue in Hessian matrix) can differentiate the types of interaction. Thus, a high value of ρ and negative sign of sign(λ_2)ρ indicates an attractive interaction, while positive sign of sign(λ_2)ρ suggests a repulsive force.

The plots of the reduced density gradient (RDG) versus sign(λ_2)ρ as well as the molecular diagrams displaying noncovalent interaction regions for AlR_3 complexes with pyrazine are illustrated in Fig. 6. These examples are demonstrative for all complexes investigated. (The remaining complexes are presented in Fig. S5).

[Insert Fig. 6 here]

Green areas appear between triel atoms and pyrazine carbon atoms / C-C bonds. However, these attractive regions are surrounded by small repulsive brown fragments which suggests a simple description as triel bond is perhaps oversimplified. Since these green/brown isosurfaces stretch into regions other than triel atoms, it is logical to conclude there are more than one π-hole interaction as well as secondary interactions.

Moving to the plots located above the diagrams, the spikes of sign(λ_2)ρ at low densities confirm the presence of a few attractive (sign(λ_2)ρ< 0) and repulsive (sign(λ_2)ρ > 0) interactions, corresponding to the green and brown isosurfaces in the molecular diagrams. The values of sign(λ_2)ρ on x axis are about 0.005-0.015 au apart from 0 in both directions. This range is characteristic for weak hydrogen bonds or weak steric repulsions as the stronger forces are characterized by values above 0.02 au [86-89].

4. DISCUSSION AND CONCLUSIONS

The results of these calculations can be compared with prior publications related to the general matter of π-hole interactions and triel bonds. The first point of comparison is derived from the recent work of Grabowski [41] involving B···N triel bonds in boron trihalide adducts with NH_3, HCN, and N_2. E_{int} reached up to -50 kcal/mol, comparable to our computed data involving pyrazine. This work also noted that Cl or I substituents on B are energetically preferable depending on the particular base. Complexes with NH_3 were the most stable, yielding interaction energies similar to our own. Importantly, this work found the same correlation between interaction and deformation energies as noted here. The higher stability of ammonia complexes was linked with greater deformation of the Lewis acid. Other works examining tetrel and triel bonds have also observed an association between monomer deformation and overall interaction energy [42-44]. As was done above, AIM analysis has also been used elsewhere [41] to categorize complexes into strong and weak categories by the total electron energy (H) which also nicely correlated with B···N distances. The values of ρ and $\nabla^2\rho$ for the strongest BCl_3···NH_3

complex were 0.131 and 0.256 au, respectively, comparable to the same quantities for the most stable BBr_3···pyrazine complex examined here.

Another work by Grabowski [44] considered B and Al π-hole donors paired with π-donors acetylene and ethylene. With only one exception, π-hole donors involving B were only marginally distorted, with E_{def} of 1.3 kcal/mol or less. These distortions were considerably higher in the Al complexes, opposite to the pattern noted here for complexes with N lone pair donor pyrazine. Nevertheless, one still sees the same association between deformation and interaction energies as well as negative values of H for the strongest complexes, in line with our own trends. As in the calculations described above, the HC≡CH and $H_2C{=}CH_2$ π-donors transfer charge into the Tr p-orbital. Some of these E(2) perturbation energies are as high as 347 kcal/mol for Tr=Al, even larger than the quantities extracted here.

The B···N triel bond was considered by Esrafili and Mousavian [45] wherein the BH_2 group is attached to a phenyl ring as a third substituent. Even though this ring cuts the intensity of the B π-hole in half, binding with NH_3 and $H_2C{=}NH$ remain strong with E_{int} of nearly 40 kcal/mol. As noted earlier [41] N_2 represents a very weak electron donor, with E_{int} barely more than 1 kcal/mol. The calculated data for two strong triel-bonded complexes were supported by large descriptors of BCPs, as well as NBO E(2) reaching over 300 kcal/mol, and a large associated CT of 320 me. These values are comparable to our own maximum quantities of 312 kcal/mol and 350 me, respectively. Other similarities to the current work derive from EDA decomposition. For stronger complexes, electrostatic and polarization terms are nearly equally dominant (about 50 and 40% of total attractive forces, respectively while for appreciably weaker complexes dispersion surges in importance to over 50%, similar to the trends reported above..

Triel-bonded complexes of BR_3 with π-donors ethene and its fluoroderivatives were recently examined by Bauza and Frontera [46]. Despite a different computational level, their MEPs are in near coincidence with our own. The π-hole intensities were ordered there according to the R substituents: F > Cl > Br, tracing the same trend and similar values of $V_{s.max}$ as computed here. The only significant difference occurs in the case of BF_3 where secondary maxima (σ-holes) were found, while no such features were observed here. With regard to triel bonded complexes, E_{int} was computed in the range of -8.2 to -28.1 kcal/mol and the intermolecular R(B··C) distances were all longer than 3 Å. These π-donors are thus less potent than the N lone pair in

pyrazine. These authors found that the triel-bonded complexes were energetically preferred over lone pair-π and halogen-π interactions.

An earlier work had calculated the thermodynamic properties of molecular complexes of Al and Ga trihalides with pyrazine and pyrimidine [90]. The pyrazine complex stability decreases in the order: $AlCl_3$ > $AlBr_3$ > $GaCl_3$ > $GaBr_3$ which is consonant with the results obtained here. Pyrimidine was found to be a more potent electron donor in these triel-bonded adducts than pyrazine, albeit by only a small margin. Other complexes of triel-hydride type between $THMe_3$ (T = Si, Ge and Sn) and TrR_3 (Z = B and Al; R = H, Me) were characterized [47] with E_{int} ranging between -2.82 and -40.59 kcal/mol. The more tightly bonded dimers were the ones with R=H rather than Me, which agrees with our results. Again, the influence of the deformation energy was involved in the stronger interactions for R=H. The MEP maxima correlated well with those quoted above. The authors found evidence that the B···H interactions in their dimers are driven mainly by electrostatics and polarization, with the latter composed largely of the σ(T-H)→LP*(Tr) donation which parallels LP(N)→LP*(Tr) transfer found in the systems described here. The CT in these complexes was quite large, exceeding 500 me and even greater than the charge transfer in our complexes..

Finally, 72 dimers stabilized by triel bonds, $R_3TH\cdots TrR_3$ (R=H, F, Cl, Me; T=Si, Ge; Tr=B, Al, Ga) were very recently characterized by Jabłoński [48]. The binding energies of complexes stabilized by B···H interactions were less than 20 kcal/mol. When B serves as the Lewis acid center, the complexes are much weaker than those in which the central atom is either Al or Ga. This finding runs counter to our own data indicating the greater strength of B as a triel center. With respect to substituents, the adducts are strongest for R=F, but only for Al and Ga complexes; this trend is reversed for Tr=B. This trend is only partly consonant with our data, all of which suggests significant differences between B···H and B···N triel bonds.

A survey of the CSD (Cambridge Structural Database) [91] provides a number of examples of crystal structures that are similar to the complexes examined here, systems stabilized by π-hole triel bonds. Several such examples [90,92] are illustrated in Fig. S6. These examples contain not only a single triel bond but also symmetrical trimers with two π-hole triel bonds engaging both pyrazine N atoms simultaneously.

In conclusion, the full picture of possible types of complexation of TrR_3 with pyrazine has been thoroughly investigated here. The optimized minima were divided into three groups: The

strongest π-hole complexes are stabilized by triel bonds to the pyrazine N lone pair for which E_{int} varies between 20.4 and 50.2 kcal/mol. The dependence of bond strength upon substituent is different for Tr=B than for its Al and Ga congeners. Weaker stacked complexes are stabilized by dispersive forces as well as several specific interactions including triel bonds. E_{int} is considerably lower here, varying between 1.4 and 8.1 kcal/mol. Several monomers can also engage in even more weakly bound dimers with pyrazine, mainly stabilized by weak H-bonds, with interaction energies of 2 kcal/mol or even less. The dependence on factors other than electrostatics is exemplified by the overall discrepancy between $V_{s,max}$ and E_{int}. The B-containing complexes are a particular example where interaction energies exceed what might be predicted based on the MEP. The orbital interaction component plays an outsized role in these adducts. The weaker stacked complexes are driven by different forces than their stronger cousins, dispersion in particular. The purported triel bonds appear to engage with the C atoms of the pyrazine ring, rather than N.

Acknowledgements

This work was financed in part by a statutory activity subsidy from the Polish Ministry of Science and Higher Education for the Faculty of Chemistry of Wroclaw University of Science and Technology. A generous computer time from the Wroclaw Supercomputer and Networking Center is acknowledged.

References

[1] L. Strekowski, B. Wilson, *Mutat. Res. Fund. Mol. Mech. Mut.* **2007**, *623*, 3.

[2] M. Barceló-Oliver, C. Estarellas, A. García-Raso, A. Terrón, A. Frontera, D. Quiñonero, I. Mata, E. Molins, P.M. Deyà, *Cryst. Eng. Comm.* **2010**, *12*, 3758.

[3] E.A. Meyer, R.K. Castellano, F. Diederich, *Angew. Chem. Int. Ed.* **2003**, *42*, 1210.

[4] L.M. Salonen, M. Ellermann, and F. Diederich, *Angew. Chem. Int. Ed.* **2011**, *50*, 4808.

[5] H.J. Schneider, *Angew. Chem. Int. Ed.* **2009**, *48*, 3924–3977.

[6] P. Hobza, K. Müller-Dethlefs, *Non-Covalent Interactions, Theory and Experiment* (Ed.: J. Hirst); Royal Society of Chemistry: Cambridge, UK, **2010**.

[7] J.-L. M. Abboud, B. Nemeth, J.-C. Guillemin, P. Burk, A. Adamson, E. R. Nerut, *Chem. Eur. J.* **2012**, *18*, 3981.

[8] A. Adamson, J.-C. Guillemin, P. Burk, *J. Phys. Org. Chem.* **2015**, *28*, 244.

[9] S. Bhunya, T. Malakar, G. Ganguly, A. Paul, *ACS Catal.* **2016**, *6*, 7907.

[10] C. W. Hamilton, R. T. Baker, A. Staubitz, I. Manners, *Chem. Soc. Rev.* **2009**, *38*, 279.

[11] P. C. Hiberty, G. Ohanessian, *J. Am. Chem. Soc.* **1982**, *104*, 66.

[12] S. J. Grabowski, *ChemPhysChem.* **2015**, *16*, 1470.

[13] S. J. Grabowski, *ChemPhysChem*. **2014**, *15*, 2985.

[14] S. J. Grabowski, *Struct. Chem.* **2017**, *28*, 1163.

[15] M.D. Esrafili, *J. Mol. Model.* **2012**, *18*, 2003.

[16] J. S. Murray, P. Lane, T. Clark, K. E. Riley, P. Politzer, *J. Mol. Model.* **2012**, *18*, 541.

[17] P. Politzer, J. S. Murray, T. Clark, *Phys. Chem. Chem. Phys.* **2010**, *12*, 7748–7758.

[18] A. Bauzá, R. Ramis, A. Frontera, *J. Phys. Chem. A* **2014**, *118*, 2827.

[19] M.D. Esrafili, F. Mohammadian-Sabet, M. Solimannejad, *Struct. Chem.* **2014**, *25*, 1197.

[20] J. S. Murray, P. Lane, T. Clark, K. E. Riley, P. Politzer, *J. Mol. Model.* **2012**, *18*, 541–548.

[21] L. M. Azofra, I. Alkorta, S. Scheiner, *Theor. Chem. Acc.* **2014**, *133*, 1586.

[22] A. Bauza, T.J. Mooibroek, A. Frontera, *ChemPhysChem.* **2015**, *16*, 2496.

[23] P. Politzer, J. S. Murray, T. Clark, *Phys. Chem. Chem. Phys.* **2013**, *15*, 11178.

[24] P. Politzer, J. S. Murray, *ChemPhysChem.* **2013**, *14*, 2145.

[25] S. Scheiner, *Int. J. Quantum Chem.* **2013**, *113*, 1609.

[26] S. Scheiner, *Acc. Chem. Res.* **2013**, *46*, 280.

[27] A. Bauzá, T.J. Mooibroek, A. Frontera, *Chem. Commun.* **2015**, *51*, 1491.

[28] A. Bauza, A. Frontera, *Angew. Chem. Int. Ed.* **2015**, *54*, 7340.

[29]A. Mukherjee, S. Tothadi, G. R. Desiraju, *Acc. Chem. Res.* **2014**, *47*, 2514.

[30] M. Iwaoka, H. Komatsu, T. Katsuda, S. Tomoda, *J. Am. Chem. Soc.* **2004**, *126*, 5309.

[31] S. Zahn, R. Frank, E. Hey-Hawkins, B. Kirchner, *Chem. – Eur. J.* **2011**, *17*, 6034.

[32] A. Bauzá, T. J. Mooibroek, A. Frontera, *Angew. Chem. Int. Ed.* **2013**, *52*, 12317.

[33] E. Alikhani, F. Fuster, B. Madebene, S. J. Grabowski, *Phys. Chem. Chem. Phys.* **2014**, *16*, 2430.

[34] A. R. Buchberger, S. J. Danforth, K. M. Bloomgren, J. A.Rohde, E.L. Smith, C. C. Gardener, J. A. Phillips, *J. Phys. Chem. B* **2013**, *117*, 11687.

[35] J. P. Wrass, D. Sadowsky, K. M. Bloomgren, C.J. Cramer, J.A. Phillips, *Phys. Chem. Chem. Phys.*, **2014**, *16*, 16480.

[36] L. Gao, Y. Zeng, X. Zhang, L. Meng, *J. Comput. Chem.* **2016**, *37*, 1321.

[37] A. Bauzá, X. García-Llinás, A. Frontera, *Chem. Phys. Lett.* **2016**, *666*, 73.

[38] R. Parajuli, *Curr. Sci.* **2016**, *110*, 495.

[39] A. Bauzá, A. Frontera, *ChemPhysChem.* **2016**, *17*, 3181.

[40] S. J. Grabowski, *Phys. Chem. Chem. Phys.* **2017**, *19*, 29742.

[41] S.J. Grabowski, *J. Comput. Chem.* **2018**, *39*, 472.

[42] S. Scheiner, *J. Phys. Chem. A* **2017**, *121*, 5561.

[43] S. J. Grabowski, *Molecules*, **2018**, *23*, 1183.

[44] S. J. Grabowski, *Molecules*, **2015**, *20*, 11297.

[45] M. Esrafili, P. Mousavian, *Mol. Phys.* **2018**, *116*, 388.

[46] A. Bauza, A. Frontera, *Theor. Chem. Acc.* **2017**, *136*, 37.

[47] J. Zhang, Y. Wei, W. Li, J. Cheng, Q. Li, *Appl. Organometal. Chem.* **2018**;*e4367*; https://doi.org/10.1002/aoc.4367.

[48] M. Jabłoński, *J. Comput. Chem.*, **2018**, doi:10.1002/jcc.25178.

[49] B. Wrackmeyer, O. L. Tok, W. Milius, A. Khan, A. Badshah, *Appl. Organometal. Chem.* **2006**, *20*, 99.

[50] B. Wrackmeyer, K. Shahid, S. Ali, *Appl. Organometal. Chem.* **2005**, *19*, 377.

[51] M. Jabłoński, *Struct. Chem.* **2017**, *28*, 1697.

[52] Q. J. Tang, Q. Z. Li, *Mol. Phys.* **2015**, *113*, 3809.

[53] M. X. Liu, H. Y. Zhuo, Q. Z. Li, W. Z. Li, J. B. Cheng, *J. Mol. Model.* **2016**, *22*, 10.

[54]D. J. Giesen, J. A. Phillips, *J. Phys. Chem. A* **2003**, *107*, 4009.

[55] J. A. Phillips, C. J. Cramer, *J. Phys. Chem. B* **2007**, *111*, 1408.

[56] J. P. Wrass, D. Sadowsky, K. M. Bloomgren, C. J. Cramer, J. A. Phillips, *Phys. Chem. Chem. Phys.* **2014**, *16*, 16480.

[57] N. Vinh-Son, S. Swinnen, M. H. Matus, M. T. Nguyen, D. A. Dixon, *Phys. Chem. Chem. Phys.* **2009**, *11*, 6339.

[58] M. P. Suh, H. J. Park, T. K. Prasad, D.-W. Lim, *Chem. Rev.* **2012**, *112*, 782.

[59] P.B. Miniyar, P.R. Murumkar, P.S. Patil, M.A. Barmade, K.G. Bothara, *Mini Rev. Med. Chem.* **2013**, *13*, 1607.

[60] C. Møller, M. S. Plesset, *Phys. Rev.*, **1934**, *46*, 618.

[61] T. H. Dunning Jr., *J. Chem. Phys.*, **1989**, *90*, 1007.

[62] F. Bulat, A. Toro-Labbe, T. Brinck, J. S. Murray, P. Politzer, *J. Mol. Model.* **2010**, *16*, 1679.
[63] K. Raghavachari, G. W. Trucks, J. A. Pople, M. Head-Gordon, *Chem. Phys. Lett.* **1989**, *157*, 479.
[64] S.F. Boys, F. Bernardi, *Mol. Phys.* **1970**, *19*, 553.
[65] E. D. Glendening, C. R. Landis, F. Weinhold, *J. Comput. Chem.* **2013**, *34*, 1429.
[66] C. Lee, W. Yang, R. G. Parr, *Phys. Rev. B*, **1988**, *37*, 785.
[67] AIMAll (Version 14.11.23), Todd A. Keith, TK Gristmill Software, Overland Park KS, USA, **2014** (aim.tkgristmill.com).
[68] G. te Velde, F. M. Bickelhaupt, E. J. Baerends, C. Fonseca Guerra, S. J. A. van Gisbergen, J. G. Snijders, T. Ziegler, Chemistry with ADF, *J. Comput. Chem.*, **2001**, *22*, 931.
[69] C. Fonseca Guerra, J. G. Snijders, G. te Velde, E.J. Baerends, *Theor. Chem. Acc.*, **1998**, *99*, 391.
[70] ADF2014, SCM, Theoretical Chemistry, Vrije Universiteit, Amsterdam, The Netherlands, http://www.scm.com.
[71] F. M. Bickelhaupt, E. J. Baerends in: *Rev. Comput. Chem.* (Eds.: K.B. Lipkowitz, D.B. Boyd), Wiley, New York, **2000**, *15*, p.1-86.
[72] T. Lu. F. Chen, *J. Comput. Chem.* **2012**, *33*, 580.
[73] T. Lu, F. Chen, *J. Mol. Graph. Model.* **2012**, *38*, 314.
[74] W. Humphrey, A. Dalke, K. Schulten, VMD: visual molecular dynamics. *J. Mol. Graph.* **1996**, *14*, 33.
[75] M. J. Frisch, G. W. Trucks, H. B. Schlegel, G. E. Scuseria, M. A. Robb, J. R. Cheeseman, G. Scalmani, V. Barone, B. Mennucci, G. A. Petersson, H. Nakatsuji, M. Caricato, X. Li, H. P. Hratchian, A. F. Izmaylov, J. Bloino, G. Zheng, J. L. Sonnenberg, M. Hada, M. Ehara, K. Toyota, R. Fukuda, J. Hasegawa, M. Ishida, T. Nakajima, Y. Honda, O. Kitao, H. Nakai, T. Vreven, J. A. Montgomery Jr., J. E. Peralta, F. Ogliaro, M. Bearpark, J. J. Heyd, E. Brothers, K. N. Kudin, V. N. Staroverov, R. Kobayashi, J. Normand, K. Raghavachari, A. Rendell, J. C. Burant, S. S. Iyengar, J. Tomasi, M. Cossi, N. Rega, J. M. Millam, M. Klene, J. E. Knox, J. B. Cross, V. Bakken, C. Adamo, J. Jaramillo, R. Gomperts, R. E. Stratmann, O. Yazyev, A. J. Austin, R. Cammi, C. Pomelli, J. W. Ochterski, R. L. Martin, K. Morokuma, V. G. Zakrzewski, G. A. Voth, P. Salvador, J. J. Dannenberg, S. Dapprich, A. D. Daniels, O. Farkas, J. B.

Foresman, J.V. Ortiz, J. Cioslowski and D.J. Fox, Gaussian 09, Gaussian, Inc., Wallingford CT, **2009**.

[76] P. Politzer, J. S. Murray, M. C. Concha, *J. Mol. Model.* **2007**, *13*, 643.

[77] G. Cavallo, P. Metrangolo, R. Milani, T. Pilati, A. Priimagi, G. Resnati, G. Terraneo, *Chem. Rev.* **2016**, *116*, 2478.

[78] W. Zierkiewicz, M. Michalczyk, S. Scheiner, *Molecules* **2018**, *23*, 6.

[79] W. Zierkiewicz, M. Michalczyk, S. Scheiner, *Phys. Chem. Chem. Phys.* **2018**, *20*, 4676.

[80] W. Zierkiewicz, M. Michalczyk, S. Scheiner, *Phys. Chem. Chem. Phys.* **2018**, *20*, 8832.

[81] W. Zierkiewicz, M. Michalczyk, *Theor. Chem. Acc.* **2017**, *136*, 125.

[82] J. Fanfrlık, W. Zierkiewicz, P. Svec, J. Rezac, M. Michalczyk, Z. Ruzickova, A. Ruzicka, D. Michalska, P. Hobza, *J. Mol. Model.* **2017**, *23*, 128.

[83] P. Scilabra, G. Terraneo, G. Resnati, *J. Fluorine Chem.* **2017**, *203*, 62.

[84] D. Cremer, E. Kraka, *Croat. Chem. Acta* **1984**, *57*, 1259.

[85] S. Jenkins, I. Morrison, *Chem. Phys. Lett.* **2000**, *317*, 97.

[86] J. Contreras-Garcia, E. R. Johnson, S. Keinan, R. Chaudret, J.-P. Piquemal, D. N. Beratan, W. Yang, *J. Chem. Theory Comput.* **2011**, *7*, 625.

[87] E. R. Johnson, S. Keinan, P. Mori-Sanchez, J. Contreras-Garcia, A. J. Cohen, W. Yang, J. Am. Chem. Soc. 2010, 132, 6498.

[88]P. Hobza, *Chem. Commun*. **2016**, *52*, 3500.

[89] E. R. Johnson, S. Keinan, P. Mori-Sanchez, J. Contreras-Garcia, A. J. Cohen, W. Yang, *J. Am. Chem. Soc.*, **2010**, *132*, 6498.

[90]T. Sevastianova, M. Bodensteiner, A. Lisovenko, E. Davydova, M. Scheer, T. Susliakova, I. Krasnova, A. Timoshkin, *Dalton Trans.*, **2013**, *42*, 11589.

[91]The Cambridge Structural Database: C. R. Groom, I. J. Bruno, M. P. Lightfoot and S. C. Ward, *Acta Cryst.* **2016**, *B72*, 171.

[92]E. Chenard, A. Sutrisno, L. Zhu, R. Assary, J. Kowalski, J. Barton, J. Bertke, D. Gray, F. Brushnett, L. Curtiss, J. Moore, *J. Chem. Phys. C*, **2016**, *120*, 8461.

TABLE 1. Values of π-hole maxima in the MEPs ($V_{s,max}$, kcal/mol) of the TrR_3 (Tr= B, Al, Ga, R = H, F, Cl, Br, CH_3) isolated molecules. Also shown in parentheses are values of secondary maxima. Data obtained at the MP2/aug-cc-pVDZ level of theory.

Triel atom (Tr)	optimized monomer				
	H	F	Cl	Br	CH_3
B	44.1	60.9	29.8 (9.8)	22.5 (14.3)	21.4 (11.4)
Al	80.2	118.8	80.4 (2.3)	68.6 (7.0)	60.1 (9.2)
Ga	65.7	101.7	72.5 (4.0)	61.0 (9.0)	49.0 (9.7)
	in geometry within dimer				
B	73.6	96.7	58.1 (9.9)	46.6 (14.8)	50.7 (11.6)
Al	102.7	159.3	117.4 (42.8)	100.8 (35.0)	84.2 (33.7)
Ga	81.9	127.7	98.1 (42.7)	84.7 (34.9)	64.7 (32.2)

TABLE 2. Interaction energy (E_{int}) corrected for BSSE, deformation energy (E_{def}) of Lewis acid and selected geometric data of Tr··N complexes with pyrazine (energies in kcal/mol, distances in Å, angles in degrees) at the MP2/aug-cc-pVDZ level of theory (E_{int} was calculated also at the CCSD(T)/aug-cc-pVDZ level using MP2 geometries).

Lewis acid	E_{int} MP2	E_{int} CCSD(T)	E_{def} (TrR_3)	ΔE [a]	R(Tr···N)	θ(Tr-N1-N4)[b]
BH_3	-43.23	-40.97	13.00	-29.91	1.633 (47)[c]	177.8
BF_3	-44.98	-44.44	24.24	-20.26	1.665 (48)	176.5
BCl_3	-49.60	-44.29	25.69	-22.82	1.642 (47)	176.7
BBr_3	-50.23	-43.99	25.06	-24.08	1.631 (47)	176.6
$B(CH_3)_3$	-33.68	-29.96	17.28	-16.25	1.675 (48)	177.8
AlH_3	-29.64	-28.66	3.66	-25.47	2.104 (62)	178.3
AlF_3	-44.09	-44.35	6.70	-37.18	2.026 (60)	179.1
$AlCl_3$	-43.61	-41.18	7.32	-36.04	2.027 (60)	175.6

$AlBr_3$	-42.33	-39.31	7.15	-34.89	2.032 (60)	175.1
$Al(CH_3)_3$	-26.51	-25.15	3.69	-22.34	2.110 (62)	176.2
GaH_3	-24.05	-22.78	3.40	-20.27	2.145 (63)	178.3
GaF_3	-41.81	-41.68	6.57	-34.88	2.049 (60)	179.7
$GaCl_3$	-38.73	-35.81	6.95	-31.21	2.056 (60)	175.7
$GaBr_3$	-36.82	-33.31	6.69	-29.56	2.063 (60)	175.1
$Ga(CH_3)_3$	-20.41	-18.79	3.14	-16.83	2.164 (63)	176.1

[a] ΔE calculated as sum of E_{int} and E_{def} (TrR_3) + E_{def} (pyrazine).
[b] θ refers to the angle between: Tr, N1 (involved in triel bond) and N4 (other N in pyrazine ring);
[c] percentage of the sum of the corresponding van der Waals radii in parentheses.

TABLE 3. EDA/BLYP-D3(BJ)/ZORA/TZ2P decomposition of the interaction energy of Tr··N lone-pair complexes of Lewis acids with pyrazine into Pauli repulsion (E_{Pauli}), electrostatic (E_{elec}), orbital interaction (E_{oi}) and dispersion (E_{disp}) terms. All energies in kcal/mol. The values in percent express the contribution of each to the sum of all attractive energy terms.

Lewis acid	E_{int}	E_{Pauli}	E_{elec}	%	E_{oi}	%	E_{disp}	%
BH_3	-45.39	120.23	-80.17	48	-81.53	49	-3.91	2
BF_3	-42.26	141.48	-96.59	53	-82.68	45	-4.47	2
BCl_3	-43.87	196.31	-118.17	49	-112.94	47	-9.08	4
BBr_3	-45.43	213.66	-124.80	48	-123.73	48	-10.55	4
$B(CH_3)_3$	-32.02	141.30	-87.25	50	-77.34	45	-8.72	5
AlH_3	-30.67	57.55	-53.39	61	-30.35	34	-4.48	5
AlF_3	-45.64	61.18	-65.26	61	-36.43	34	-5.14	5
$AlCl_3$	-43.65	84.61	-74.25	58	-45.54	36	-8.47	7
$AlBr_3$	-42.47	91.54	-76.04	57	-48.36	36	-9.60	7
$Al(CH_3)_3$	-27.25	64.91	-54.90	60	-29.30	32	-7.96	9
GaH_3	-23.28	67.65	-56.60	62	-29.79	33	-4.54	5
GaF_3	-39.85	86.34	-78.33	62	-42.72	34	-5.14	4
$GaCl_3$	-34.61	105.11	-82.69	59	-48.62	35	-8.41	6
$GaBr_3$	-32.72	110.72	-83.50	58	-50.38	35	-9.56	7
$Ga(CH_3)_3$	-18.90	72.80	-55.89	61	-27.83	30	-7.97	9

TABLE 4. NBO values of sum of the E(2) for LP(N)→σ*(Tr-R), and LP(N)→LP*(Tr) orbital interactions (in kcal/mol) and total charge transfer (CT, in me) from pyrazine to TrR_3 in Tr··N lone pair bonded complexes obtained at the BLYP-D3(BJ)/def2-TVZPP level.

Lewis acid	Σ LP(N)→σ*(Tr-R)	LP(N)→ LP*(Tr)	CT
BH_3	2.11	301.51	304
BF_3	5.61	245.86	315
BCl_3	5.18	312.34	350
BBr_3	4.59	299.14	321
$B(CH_3)_3$	2.42	254.95	303
AlH_3	9.72	62.31	133
AlF_3	-	91.36	126
$AlCl_3$	-	99.64	139
$AlBr_3$	-	95.28	130
$Al(CH_3)_3$	-	81.74	106
GaH_3	8.94	62.41	148
GaF_3	-	94.22	152
$GaCl_3$	-	117.17	166
$GaBr_3$	15.39	66.20	159
$Ga(CH_3)_3$	10.57	54.02	112

TABLE 5. AIM results for theTr··N lone pair bonded TrR_3 complexes with pyrazine. Bond critical point (BCP) properties: electron density ρ, Laplacian of electron density $\nabla^2\rho$ (both in atomic units) and total electron energy (H, kcal mol^{-1}). Calculations were performed at the MP2/aug-cc-pVDZ level.

pyrazine···system	interaction	ρ	$\nabla^2\rho$	H
BH_3	B···N	0.099	0.613	-25.99
BF_3	B···N	0.106	0.352	-41.28

BCl_3	B···N	0.116	0.379	-47.08
	Cl···H	0.017	0.063	1.12
BBr_3	B···N	0.119	0.398	-48.50
	Br···H	0.018	0.057	0.75
$B(CH_3)_3$	B···N	0.090	0.535	-24.09
	C···H	0.013	0.061	1.76
AlH_3	Al···N	0.040	0.258	3.36
AlF_3	Al···N	0.049	0.337	4.73
$AlCl_3$	Al···N	0.051	0.335	3.63
	Cl···H	0.010	0.035	0.80
	Cl···H	0.010	0.035	0.80
$AlBr_3$	Al···N	0.051	0.328	3.27
	Br···H	0.011	0.033	0.64
	Br···H	0.010	0.033	0.66
$Al(CH_3)_3$	Al···N	0.039	0.252	3.09
GaH_3	Ga···N	0.059	0.255	-6.28
GaF_3	Ga···N	0.075	0.345	-8.43
$GaCl_3$	Ga···N	0.075	0.335	-8.92
	Cl···H	0.010	0.334	0.75
	Cl···H	0.010	0.335	0.75
$GaBr_3$	Ga···N	0.075	0.324	-9.03
	Br···H	0.010	0.032	0.61
	Br···H	0.010	0.032	0.61
$Ga(CH_3)_3$	Ga···N	0.056	0.240	-6.12

TABLE 6. Interaction energy (E_{int}) corrected for BSSE, deformation energy (E_{def}) of Lewis acid and selected geometric data of stacked complexes with pyrazine (energies in kcal/mol, distances in Å, angles in degrees) at the MP2/aug-cc-pVDZ level of theory (E_{int} was calculated also at the CCSD(T)/aug-cc-pVDZ level using MP2 geometries).

Lewis acid	E_{int} MP2	E_{int} CCSDT	E_{def} (TrX_3)	ΔE MP2	R(Tr···N)[a]	R(Tr···C-C)[b]
BH_3	-3.11	-2.06	0.23	-2.88	3.249 (94)[c]	2.587
BF_3	-1.38	-1.08	0.05	-1.33	3.275 (94)	3.035
BCl_3	-3.39	-1.59	0.03	-3.36	3.490 (101)	3.250
BBr_3	-3.70	-1.43	0.03	-3.67	3.486 (100)	3.263
$B(CH_3)_3$	-3.89	-2.36	0.42	-3.47	3.386 (98)	3.066
AlH_3	-4.25	-3.49	0.29	-3.96	3.319 (98)	2.810
AlF_3	-7.69	-7.88	2.20	-5.49	2.960 (87)	2.639
$AlCl_3$	-7.71	-5.38	2.40	-5.31	3.028 (89)	2.740
$AlBr_3$	-7.10	-4.24	2.14	-4.96	3.082 (91)	2.786
$Al(CH_3)_3$	-4.97	-3.47	0.28	-4.69	2.897 (85)	3.526
GaH_3	-3.69	-2.66	0.27	-3.42	3.398 (99)	2.769
GaF_3	-8.14	-8.16	2.65	-5.49	2.971 (87)	2.570
$GaCl_3$	-6.96	-4.34	2.55	-4.41	3.042 (89)	2.711
$GaBr_3$	-6.20	-3.07	2.19	-4.01	3.097 (91)	2.766
$Ga(CH_3)_3$	-4.52	-2.72	0.40	-4.12	3.395 (99)	2.837

[a] distance between Tr atom and closest N atom from the ring;
[b] distance between Tr atom and closest C-C midpoint;
[c] percentage of the sum of the corresponding van der Waals radii in parentheses.

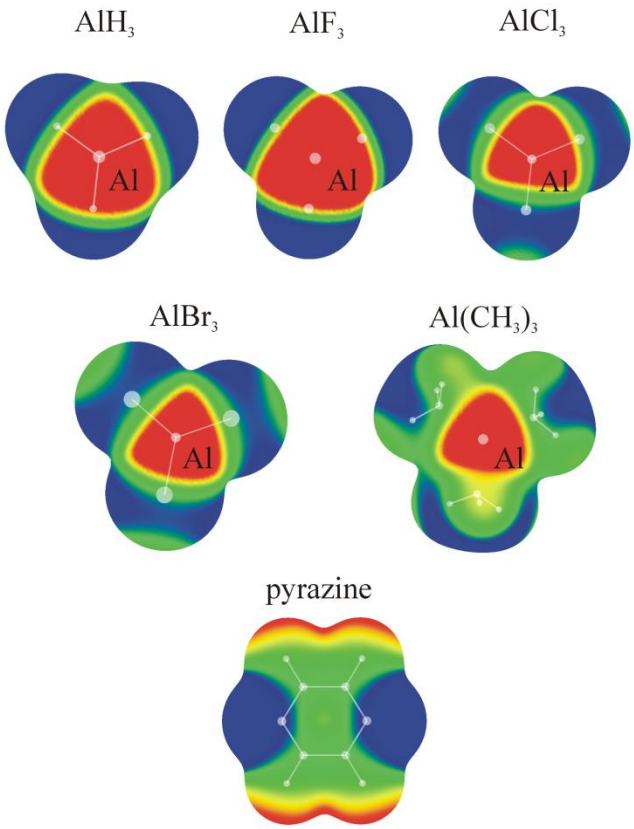

Fig. 1. MEPs of AlR_3 (R = H, F, Cl, Br, CH_3) isolated molecules as π-hole donors, computed on the 0.001 au isodensity surface at the MP2/aug-cc-pVDZ level. Also shown is the MEP of pyrazine. Colour ranges, in kcal/mol, are: red greater than 15, yellow between 8 and 15, green between 0 and 8, blue below 0 kcal/mol.

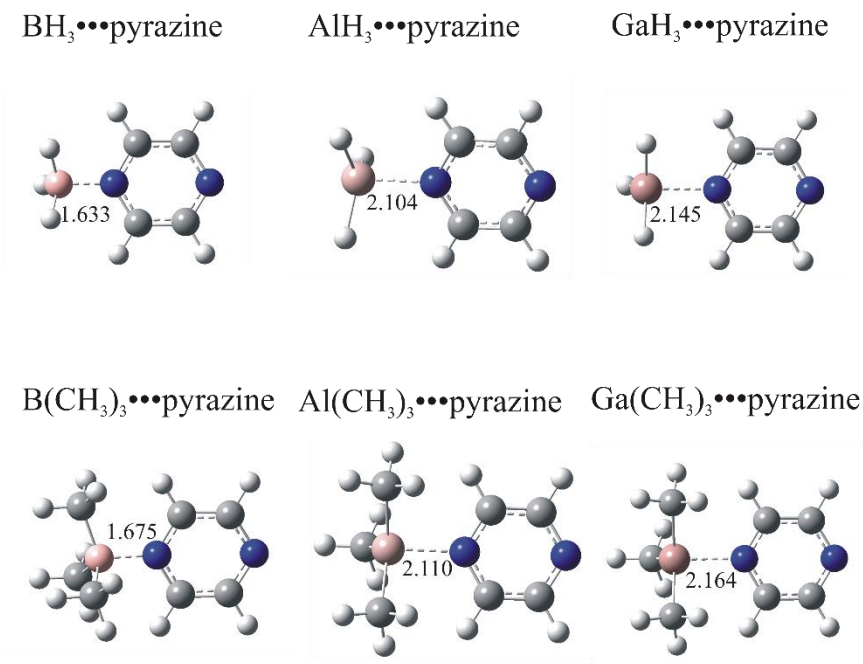

Fig. 2. MP2/aug-cc-pVDZ optimized structures of TrH_3 and $TrMe_3$ complexes with pyrazine. Distances in Å.

$AlH_3\cdots$pyrazine	
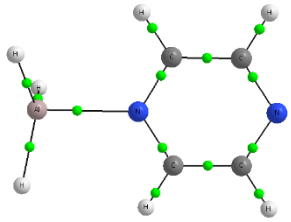	
$AlF_3\cdots$pyrazine	$AlCl_3\cdots$pyrazine
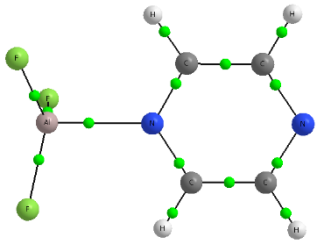	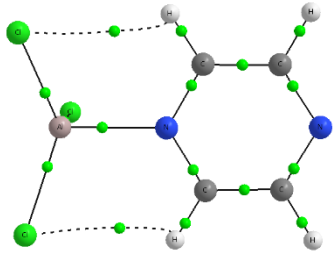
$AlBr_3\cdots$pyrazine	$Al(CH_3)_3\cdots$pyrazine

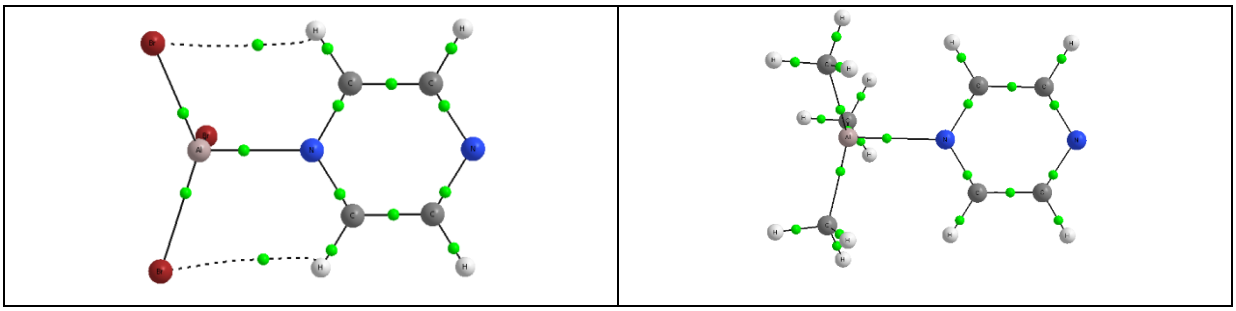

Fig. 3 AIM diagrams showing bond critical points (green dots) in Al-containing complexes stabilized by Tr··N triel bonds.

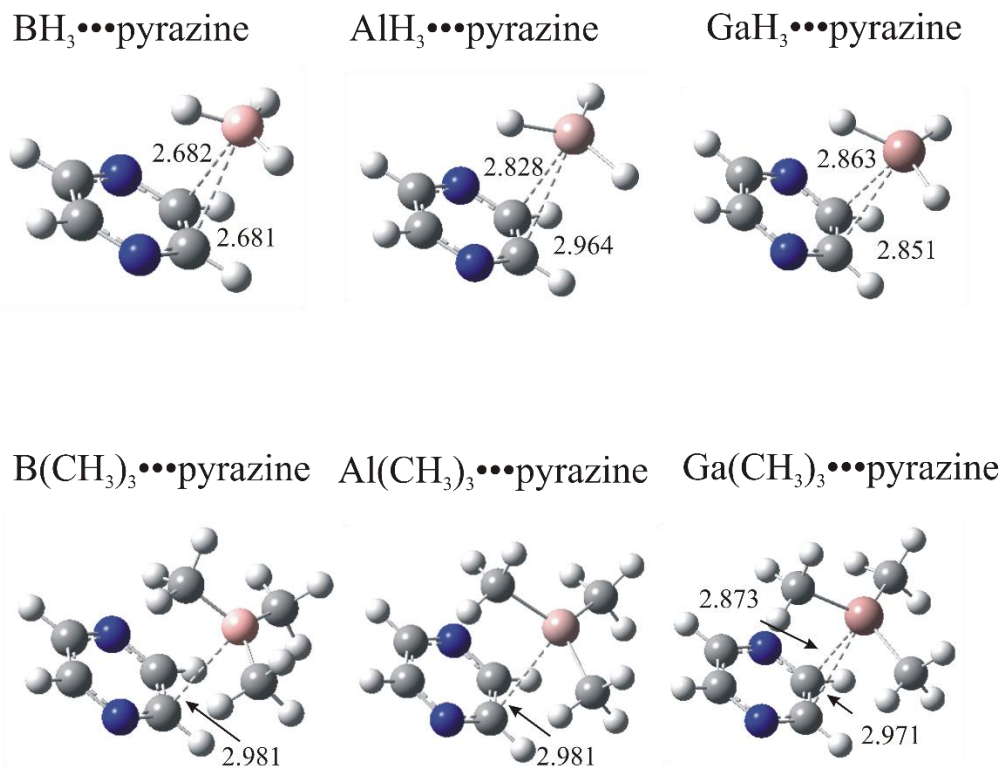

Fig. 4. MP2 optimized structures of stacked TrH_3 and $TrMe_3$ complexes with pyrazine. Calculations performed at the MP2/aug-cc-pVDZ level. Distances in Å.

$AlH_3\cdots$pyrazine	
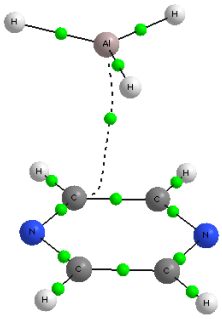	
$AlF_3\cdots$pyrazine	$AlCl_3\cdots$pyrazine
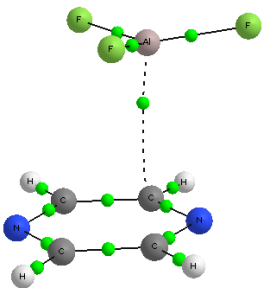	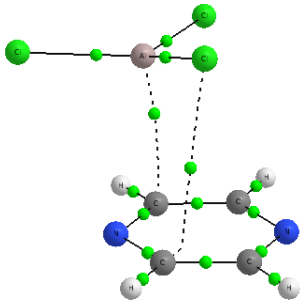
$AlBr_3\cdots$pyrazine	$Al(CH_3)_3\cdots$pyrazine
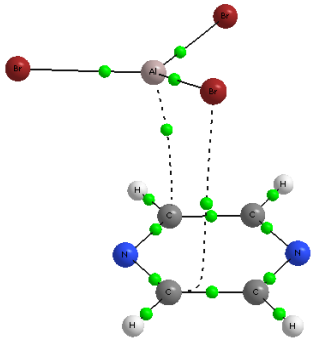	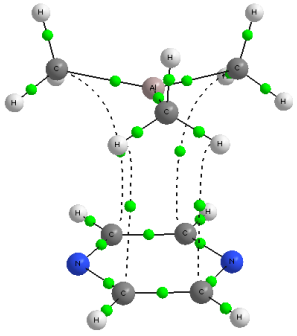

Fig. 5 AIM diagrams showing the bond critical points (green dots) in Al-containing stacking complexes with pyrazine stabilized by π-hole triel bonds.

AlH_3···pyrazine	AlF_3···pyrazine	
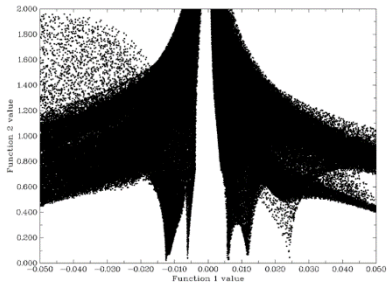	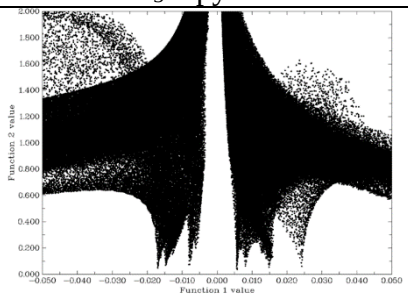	
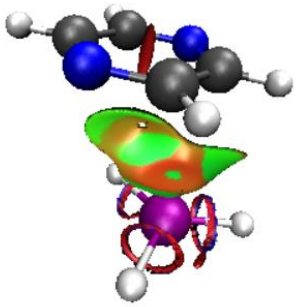	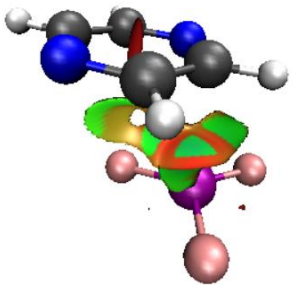	
$AlCl_3$···pyrazine	$AlBr_3$···pyrazine	$Al(CH_3)_3$···pyrazine
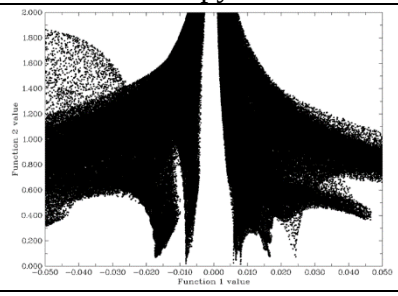	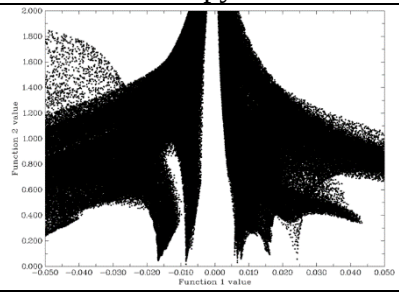	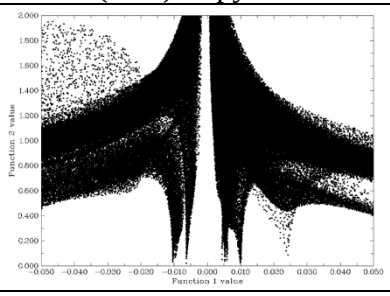
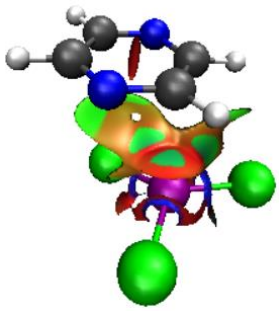	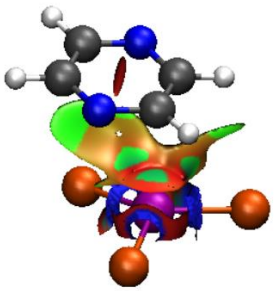	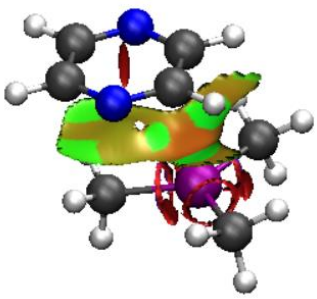

Fig. 6. Plots of the reduced density gradient (RDG) versus sign $(\lambda_2)\rho$ for the illustrative Al-containing stacked complexes with pyrazine. Al atoms are purple. Bonding isosurfaces are green and blue disks while brown and red areas represent weak and strong repulsive forces, respectively.)